ELSEVIER

Surface Science 411 (1998) L783–L788

surface science

Surface Science Letters

# Quantum diffusion of hydrogen and deuterium on nickel (100)

Roi Baer [a], Yehuda Zeiri [b], Ronnie Kosloff [c]

[a] *Department of Chemistry, University of California Berkeley and Chemical Sciences Division, Lawrence Berkeley National Laboratories, Berkeley, CA 94720, USA*
[b] *Department of Chemistry, Nuclear Research Center-Negev, Beer-Sheva, 84190, PO Box 9001, Israel*
[c] *Department of Physical Chemistry and the Fritz Haber Research Center, The Hebrew University, Jersusalem 91904, Israel*

Received 29 December 1997; accepted for publication 14 April 1998

**Abstract**

The diffusion constants of hydrogen and deuterium at low temperature are calculated using the surrogate Hamiltonian method and an embedded atom potential. A comparison with previous experimental and theoretical results is made. A crossover to temperature-independent tunneling occurs at 69 K for hydrogen and at 46 K for deuterium. An inverse isotope effect at intermediate temperatures is found, consistent with experiment. Deviations are found at low temperature where a large isotope effect is calculated.


*Keywords:* Ab initio quantum chemical methods and calculations; Computer simulations; Construction and use of effective interatomic interactions; Diffusion and migration; Hydrogen; Low index single crystal surfaces; Nickel; Single crystal surfaces

The dynamics of adsorbed hydrogen atoms on metal surfaces at low temperatures is of fundamental theoretical interest. This is because of the complex character of the interaction of hydrogen with the many degrees of freedom of the metal and the quantum nature of the hydrogen motion at low temperatures, dominated by tunneling. New experimental techniques have been applied to measure hydrogen and deuterium diffusion on the surfaces of tungsten [1,2] and nickel [3–6]. For high temperatures the diffusion constants had an Arrhenius form [7,8] characterized by an activation energy and a pre-exponential factor. The low temperature experimental results showed that at around 100 K the diffusion constants were almost temperature independent, implying that quantum tunneling is predominant. Two other interesting results were observed when diffusion of deuterium and hydrogen was compared. The pre-exponential factor of the diffusion constant of deuterium was substantially higher than that of hydrogen. This effect is an inverse isotope effect. Second, in the low temperature tunneling regime the diffusion constants of the two isotopes were similar.

Several theoretical attempts [3,9–11] have been made for resolution of these results for the hydrogen tungsten system. One approach [3,9] was based on the Flynn–Stoneham [12] theory of diffusion of light interstitials. As noted by Sethna [13], this theory makes an adiabatic separation, assuming hydrogen is fast and metal atoms slow, inappropriate for this system. Indeed, exact calculations on a two-dimensional tunneling model showed that this approximation can lead to underestimation of tunneling rates by orders of magnitude [14]. When applied to deuterium, the model

0039-6028/98/$ see front matter 
PII: S0039-6028(98)00322-7

becomes worse. A mass renormalization approach was developed by Muttalib and Sethan [10] and applied to the hydrogen–tungsten diffusion system. Here the hydrogen was assumed to be slow compared with the phonon modes, which is also questionable.

Mattsson et al. [15,16] and Wonchoba et al. [17] have studied in detail the hydrogen–nickel system using different dynamical methods. In both these studies the metal–metal and hydrogen–metal interactions were modeled by an embedded atom semi-empirical potential. Mattsson et al. [15,16] used a path centroid method [18,19] for the dynamical transport calculations. In these calculations the substrate nickel atoms were first treated classically while the hydrogen or deuterium motion was quantal. An additional calculation was attempted to correct for quantum effects of the nickel motion by assuming an interaction linear in both the heavy atom and the hydrogen atom displacements. It was found that the quantum nature of the bath has a marked effect on the tunneling rates.

Wonchoba et al. have recently published two semiempirical EAM [20] potential functions (named EAM5 in Ref. [17] and EAM6 in Ref. [21]) with increasing precision for the hydrogen–nickel interactions. These have been carefully constructed to reproduce closely a variety of empirical data measured for nickel (bulk and surface) and for the hydrogen–nickel interactions. Based on these potentials, they studied the diffusion constant and its thermal dependence for hydrogen. The dynamical method they developed was the canonical variational transition-state theory with small curvature tunneling (SCT) corrections based on quantized reactant states. The calculated results were again in quantitative disagreement with experiments, although much closer than those reported by Mattsson et al. [16]. Wonchoba et al. did not, however, address in their work the issue of isotope effects in this system.

The surrogate Hamiltonian method [22] is especially designed for low temperature quantum dynamics of light interstitials in condensed phases. This procedure is fully quantal, treating the metal degrees of freedom as quantum baths of harmonic oscillators, where the structure of the baths and the approximate interaction of the hydrogen atom with it is extracted from a classical-dynamical simulation. This study reports calculations of the low temperature diffusion constant of hydrogen on a surface of nickel, using the potential function EAM5 of Wonchoba et al. [17].

A detailed account of the calculations will be published shortly, here only the main points of the theory are outlined. Given the full interaction potential of the system, we construct a model Hamiltonian of the general form:

$$H = \frac{P^2}{2M} + v_{\mathrm{eff}}(R) + \sum_{n,k} \epsilon_n b_n^{+} b_n + \sum_n V_n(R)(b_n^{+} + b_n). \tag{1}$$

The primary tunneling motion is described by a one-dimensional particle of mass $M$ (equal to the isotope mass) with Cartesian position coordinate $R$ and the conjugate momentum $P$, moving in an adiabatic potential $v_{\mathrm{eff}}(R)$ and coupled to a bath of modes representing the vibrations of the metal atoms (and the two additional orthogonal degrees of freedom of the hydrogen). The bath modes are labeled by a set of quantum numbers $n$, bosonic annihilation and creation operators $b_n$, $b_n^{+}$ and excitation energies $\epsilon_n = \beta\omega_n$. Each mode is linearly coupled to the hydrogen degree of freedom by an interaction strength $V_n(R)$ which is assumed separable:

$$V_n(R) = f(R)U_n. \tag{2}$$

It can be shown [22] that the dynamics of the tunneling degree of freedom $R$ is governed by a surrogate Hamiltonian of the form:

$$H = \frac{P^2}{2M} + v_{\mathrm{eff}}(R) + \int_0^\infty \frac{\epsilon}{2} B^{+}(\epsilon)B(\epsilon)\,d\epsilon + f(R)\int_0^\infty \sqrt{J(\epsilon)}(B^{+}(\epsilon) + B(\epsilon))\,d\epsilon \tag{3}$$

where $B(\epsilon)$, $B^{+}(\epsilon)$ are boson creation and annihilation operators with $[B^{+}(\epsilon), B(\epsilon')] = \delta(\epsilon - \epsilon')$ the spectral function $J(\epsilon)$ is:

$$J(\epsilon) = \sum_n |U_n|^2 \delta(\epsilon_n - \epsilon). \tag{4}$$

The dynamics is thus determined by the potential $v_{eff}(R)$, the spectral function $J(\epsilon)$, the coupling function $f(R)$ and the high frequencies which contribute to the zero-point energy. While the only high frequency modes are those of the hydrogen itself and can be determined by examining the potential surface of hydrogen, the effective potential, spectral function, and coupling function need some more elaborate calculations. These three entities are determined using a classical simulation of the system in the full EAM5 potential of Wonchoba et al. [17]. During the simulation $R$ was kept constant, and the simulation was repeated for several values of $R$. The Ni(100) surface was represented by two moveable layers of 25 atoms. The bottom layer was coupled to two additional layers of atoms fixed at their lattice points. Periodic boundary conditions were imposed along directions parallel to the surface. The thermal coupling of the slab to the rest of the crystal was imposed by attachment of 25 fictitious particles to the bottom moveable layer. The simulation temperature was $T = 90$ K. In comparison with results of a simulation at $T = 60$ K, small shifts were found in frequency and amplitude of the spectral density, indicating that the commonly accepted harmonic approximation may not be appropriate in this system.

During the classical motion, the potential energy $V(R,t)$ of the system and the instantaneous force $F(R,t) = -\mathrm{d}V/\mathrm{d}R$ determine the effective potential:

$$V_{eff}(R) = \langle V(R,t)\rangle + [f(R)]^2 \int_0^{\infty} \frac{J(\epsilon)}{\epsilon}\,\mathrm{d}\epsilon + C(T) \tag{5}$$

where $C(T)$ depends on the temperature but not on $R$ and is excluded from the calculation. The functions $J(\epsilon)$ and $f(R)$ are determined from the Fourier transform of the autocorrelation $\langle F(R,t)F(R,0)\rangle$. Some aspects of this method are described in Ref. [22], and a complete account will be given in a future publication. The classical MD simulation spanned a time of 10 ps. Of these, the first 9 ps served as a thermalization stage and only data from the last picosecond was used to determine the spectral density and the effective potential.

The resulting spectral function can be represented as a sum of seven Gaussians:

$$J(\epsilon) = \sum_{n=1}^{7} A_n \exp\left[-\frac{(\epsilon - \nu_n)^2}{2\sigma_n^2}\right] \tag{6}$$

where the parameters $A_n$, $\nu_n$ and $\sigma_n$ are given in Table 1. The coupling function $f(R)$ is shown in Fig. 1.

Only one hydrogen degree of freedom is explicitly represented; the two high frequency perpendicular degrees of freedom of the hydrogen atom have an adiabatic effect [23] so their zero-point energy is added to the hydrogen reaction path potential $v_{eff}$. Owing to the isotopic mass difference, the adiabatic correction is dependent on the isotope, and it was found that hydrogen has a higher barrier for tunneling than deuterium.

Table 1
Parameters for the spectral function

| $n$ | $\nu_n$ (cm−1) | $A_n$ (au) | $\sigma_n$ (cm−1) |
|---|---|---|---|
| 1 | 65.0 | $1.5 \times 10^{-2}$ | 3.0 |
| 2 | 124.0 | $7.0 \times 10^{-4}$ | 14.0 |
| 3 | 151.0 | $5.7 \times 10^{-3}$ | 4.1 |
| 4 | 190.0 | $2.6 \times 10^{-3}$ | 3.0 |
| 5 | 222.0 | $6.6 \times 10^{-3}$ | 4.3 |
| 6 | 280.0 | $4.0 \times 10^{-4}$ | 13.0 |
| 7 | 345.0 | $6.0 \times 10^{-4}$ | 2.0 |

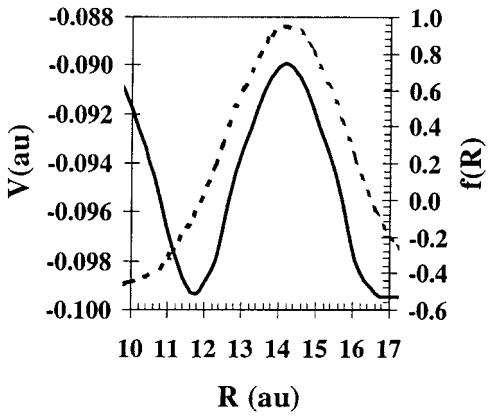


Fig. 1. The coupling function $f(R)$ superimposed on the potential $v_{eff}(R) + \sum 1/2(\epsilon_n)$. Both functions are symmetrical around $R = 14.2$ au.

However, this is partially compensated by the higher zero-point energy of hydrogen inside the metastable well (see also Fig. 3).

The calculation of the low temperature tunneling dynamics proceeds by representing the $R$ coordinate using a grid [24] and each bath mode by its $v = 0$ and $v = 1$ states. Details as to how to sample the infinite bath by a finite number of two-level systems are described in Ref. [22].

The dynamical calculations were sufficiently converged by a 4-mode bath ($N = 4$). Convergence was checked by comparing to results of a 3-mode bath and some result of a 5-mode bath. The low lying tunneling states require high accuracy representation of the $R$ coordinate.

The grid spacing was reduced until convergence. For hydrogen, a spacing of $\Delta R = 0.055$ au was used for the slowest 16 tunneling states and $\Delta R = 0.11$ au for the rest of the states. For deuterium $\Delta R = 0.028$ au was used for the 32 slowest states and $\Delta R = 0.055$ au for other states. Outgoing boundary conditions were imposed using a negative imaginary potential with potential height 0.007 au and the tunneling rate was calculated by the time–energy filter method described in Ref. [14].

By calculating the discrete tunneling spectrum of hydrogen and deuterium and thermally averaging the rates we determined the thermal diffusion rate as shown in Fig. 2. At low temperatures the diffusion constant is almost temperature independent. At high temperatures the rate converges to an exponentially increasing Arrhenius behavior. Between these two extremes lies a crossover regime. The calculated crossover temperature is 69 K for hydrogen and 45 K for deuterium. These values should be compared with experiment and other calculation, as shown in Table 2.

The diffusion rates exhibit large isotope effects at temperatures below 80 K, and become similar at higher temperatures. We suspect that the small isotope effect seen in experiments is due to the limited experimental temperature range (greater than 80 K).

The activation energy $E_a = -\mathrm{d}\ln D/\mathrm{d}\beta$, where $\beta^{-1} = k_B T$, is shown in Fig. 3 for both isotopes. At very low temperatures the activation energy is very small in magnitude, initially rising slowly with

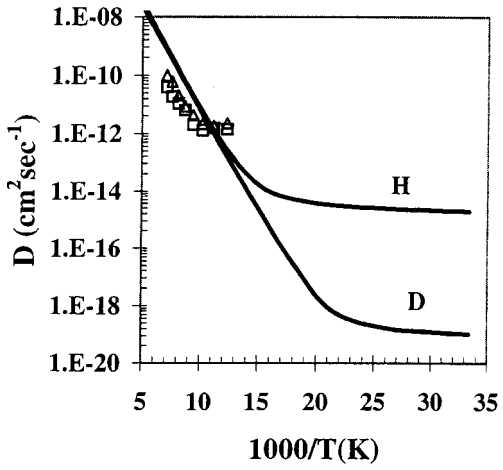


Fig. 2. Diffusion constant rates of H and D on Ni (100). Also shown, the experimental low coverage results of Lin and Gomer [3] for H (%) and D (6) on this surface.

temperature. In the crossover regime (just under 69 K for hydrogen and 45 K for deuterium) the activation energy increases rapidly. The change is very abrupt for deuterium, and more moderate for hydrogen. At higher temperatures the activation energies again becomes almost temperature independent, corresponding to an Arrhenius behavior. The high temperature activation energy approaches 3.5 kcal mol−1 for hydrogen and 3.3 kcal mol−1 for deuterium. These are within the range of reported experimental values for hydrogen (in kcal mol−1): 3.2 (Ref. [3]), 3.5 (Ref. [5]), 3.5 (Ref. [7]) and 4.0 (Ref. [8]) and for deuterium 3.6 (Ref. [3]) 5.0 (Ref. [5]) and 4.4 (Ref. [7]).

The complementary Arrhenius quantity to the activation energy is the pre-exponential factor $D_0 = D(T)\exp(E_a/k_B T)$. The isotopic ratio $D_0^a(\mathrm{D})/D_0(\mathrm{H})$ is shown in Fig. 4. The ratio shoots up from a minute value of $10^{-4}$ at temperatures of about 40 K to a huge ratio of $5 \times 10^6$ at 65 K, where it then decays as the temperature is further raised. The large inverse isotope effect, reported by various experimental studies of hydrogen diffusion on metal surfaces [2,3,5,7], by which $D_a(\mathrm{D})/D_0(\mathrm{H}) \gg 1$, is clearly seen here. In addition, we point out the strong dependence on temperature at low temperatures.

The detailed dynamical calculation presented in this work exhibits some of the peculiarities found

Table 2
Comparison of calculated and measured quantities

| | Ref. [16] (theo.) | Ref. [17] (theo.) | Present (theo.) | Ref. [3] (exp.) | Ref. [5] (exp.) |
|---|---|---|---|---|---|
| $T_c^0$(H) a | 40 | 66 | 69 | 100 | 160 |
| $T_c^0$(D) b | 25 | NA | 45 | 100 | 170 |
| $D_T^I$(H) c | $1\times10^{-18}$ | $1\times10^{-14}$ | $2\times10^{-15}$ | $2\times10^{-12}$ | $2\times10^{-11}$ |
| $D_T^I$(D) d | $1\times10^{-30}$ | NA | $2\times10^{-20}$ | $2\times10^{-12}$ | $2\times10^{-11}$ |
| $E_a^I$(H) e | NA | 4 | 3.5 | 3.2 | 3.5 |
| $E_a^I$(D) f | NA | NA | 3.3 | 3.6 | 5.0 |

a Crossover temperature for H (K).
b Crossover temperature for D (K).
c Low temperature diffusion constant for H ($cm^2\,s^{-1}$).
d Low temperature diffusion constant for D in ($cm^2\,s^{-1}$).
e High temperature activation energy for H (kcal $mol^{-1}$).
f High temperature activation energy for D (kcal $mol^{-1}$).

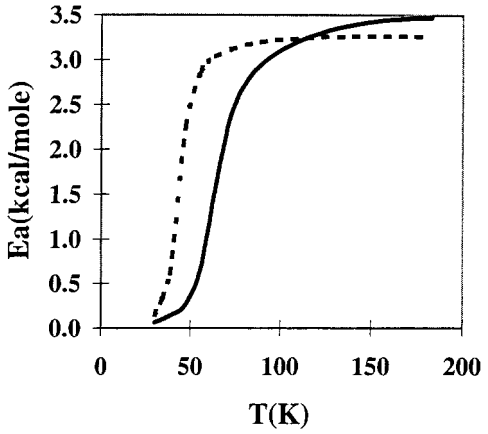


Fig. 3. The activation energy as a function of surface temperature for hydrogen (full line) and deuterium (dotted line).

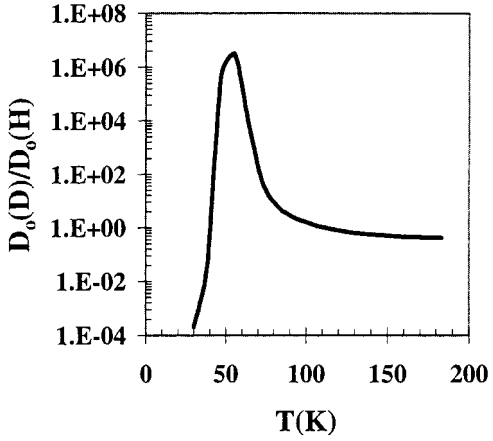


Fig. 4. The ratio of pre-exponential factors of hydrogen and deuterium as a function of temperature. The horizontal line is the classical TST ratio.

in the experiments. We found a temperature-independent diffusion regime at low temperatures, a crossover region and an Arrhenius regime at higher temperatures. The Arrhenius activation energies were found to agree with experiment. Our calculation show an inverse isotope effect, as was reported for the hydrogen–metal systems. However, our results point out that the magnitude of the effect is very sensitive to the temperature.

Here, as in previous theoretical studies [16,17], important discrepancies between experiment and theories are still unresolved:

(1) The calculated crossover temperature is lower than measured.
(2) Calculated low temperature diffusion constants show a large isotope effect, unseen in the measurements.
(3) The calculated low temperature diffusion constant is much lower than the measured one.

The discrepancy between the theoretical results and experiment may be due to an experimental problem, an issue recently raised by Zhu [25] and clearly warrants refined experimental data. The discrepancy may be attributed to the interaction potential, but recently published estimates by Mattsson et al. [26] reflect the same type of discrepancies for an ab initio potential. We have

found that the harmonic approximation may require refinement since the spectral density is temperature dependent. Another refinement may be in a multi-bath construction which has a stronger dissipative effect [14]. It therefore seems that these phenomena require more experimental and theoretical work for a clear and consistent understanding.

## Acknowledgements

This work was supported by the Israel Science Foundation. R.B. wishes to thank D. Neuhauser for enlightening discussions.

## References

[1] R. DiFoggio, R. Gomer, Phys. Rev. B 25 (1982) 3490.
[2] S.C. Wang, R. Gomer, J. Chem. Phys. 83 (1985) 4193.
[3] T.S. Lin, R. Gomer, Surf. Sci. 255 (1991) 41.
[4] X.D. Zhu, A. Lee, A. Wong, U. Linke, Phys. Rev. Lett. 68 (1992) 1862.
[5] A. Lee, X.D. Zhu, L. Deng, U. Linke, Phys. Rev. B 46 (1992) 154782.
[6] A. Lee, X.D. Zhu, L. Deng, U. Linke, Phys. Rev. B 48 (1993) 11256.
[7] D.R. Mullins, B. Roop, S.A. Costello, J.M. White, Surf. Sci 186 (1986) 67.
[8] S.M. George, A.M. DeSantolo, R.B. Hall, Surf. Sci. 159 (1985) l425.
[9] A. Auerbach, K.F. Freed, R. Gomer, J. Chem. Phys. 86 (1987) 2356.
[10] K. Muttalib, J. Sethna, Phys. Rev. B 32 (1985) 3462.
[11] K.F. Freed, J. Chem. Phys. 82 (1984) 5264.
[12] C.P. Flynn, A.M. Stoneham, Phys. Rev. B 1 (1970) 3966.
[13] J.P. Sethna, Phys. Rev. B 25 (1982) 5050.
[14] R. Baer, Y. Zeiri, R. Kosloff, Phys. Rev. B 55 (1997) 10952.
[15] T.R. Mattsson, U. Engberg, G. Wahnstrom, Phys. Rev. Lett. 71 (1993) 2615.
[16] T.R. Mattsson, G. Wahnstrom, Phys. Rev. B 51 (1995) 1885.
[17] S.E. Wonchoba, W.-P. Hu, D.G. Truhlar, Phys. Rev. B 51 (1995) 9985.
[18] G.A. Voth, D. Chandler, W.H. Miller, J. Chem. Phys. 91 (1989) 7749.
[19] G.A. Voth, Adv. Chem. Phys. 93 (1996) 135.
[20] M.S. Daw, M.I. Baskes, Phys. Rev. B 29 (1984) 2541.
[21] S.E. Wonchoba, D.G. Truhlar, Phys. Rev. B 53 (1996) 11222.
[22] R. Baer, R. Kosloff, J. Chem. Phys. 106 (1997) 8862.
[23] R.A. Marcus, J. Chem. Phys. 83 (1979) 204.
[24] R. Baer, Y. Zeiri, R. Kosloff, Phys. Rev. B 54 (1996) R5287.
[25] G.X. Cao, E. Nabighian, X.D. Zhu, Phys. Rev. Lett. 79 (1997) 3696.
[26] T.R. Mattsson, G. Wahnstrom, L. Bengtsson, B. Hammer, Phys. Rev. B 56 (1997) 2258.